

# MULTICOMPONENT DISCHARGE DYNAMICS OF ADSORBED NATURAL GAS STORAGE SYSTEMS

José P. B. Mota

Departamento de Química, Faculdade de Ciências e Tecnologia, Universidade Nova de Lisboa,  
2825 Monte de Caparica, Portugal

## ABSTRACT

Adsorption storage on highly microporous activated carbon is the most promising low-pressure alternative for storing natural gas. A detailed mathematical model has been developed in order to study the impact of natural gas composition on cycling efficiency of adsorption storage systems. Results show that net deliverable capacity is substantially decreased by heavy hydrocarbons which are present in small amounts in natural gas. Economical means of removing them from the gas stream before charge need to be identified and evaluated.

## INTRODUCTION

Natural gas (NG) has always been considered a potentially attractive fuel for vehicle use. It is cheaper than gasoline and diesel, the technical feasibility of NG vehicles is well established, and they have a less adverse effect on the environment than liquid-fueled vehicles. For example, NG can be burnt in such a way as to easily minimize  $\text{NO}_x$  and CO emissions [1]. In fact, NG outperforms petroleum based fuels in every aspect except on-board storage [2].

A large effort has been devoted to replacing NG high-pressure compression by an alternative storage method working at pressures up to 3.5 MPa. Besides allowing the use of lighter and safer on-board storage reservoirs, this upper pressure limit is easily achieved with a single-stage compressor or, alternatively, the vehicle can be refueled directly from a high-pressure pipeline. As a result, a significant decrease in the capital and operating costs of refuelling stations would be obtained.

A general consensus has been reached regarding adsorption as the most promising low-pressure alternative for storing NG. Extensive experimental work has shown that highly microporous activated carbon is the adsorbent best suited for his task. Quinn and co-workers [1] have given a detailed review of the subject and an update will be published soon [3].

Several operational problems that influence the success of adsorbed natural gas (ANG) storage have been addressed in the literature [1,2]. The one of concern here is the storage capacity loss due to the gradual contamination of the adsorbent with hydrocarbons higher than methane, which are present in trace amounts in NG. If these are not removed from the gas stream before charge, they can adsorb preferentially to high equilibrium residual levels and substantially decrease the net deliverable capacity. This is a consequence of their higher adsorption potential and of the infeasibility of operating an on-board storage reservoir at sub-atmospheric pressures.

Although some work, both analytical and experimental, has been conducted to design and test economical means of controlling the contaminants [4], very little effort has been devoted to the study of their impact on cycling efficiency. This has prompted the author to conduct the work presented here.

## PROBLEM FORMULATION

In order to assess the impact of NG composition on net deliverable capacity, the dynamic behaviour of an on-board storage cylinder is modeled as a series of consecutive cycles, each consisting on charge with a fixed gas mixture followed by discharge at constant molar rate until depletion pressure is reached.

### *Gas adsorption.*

Multicomponent adsorption equilibrium is predicted by a formalism combining Adsorption Potential [5] and Ideal Adsorbed Solution (IAS) [6] theories. The same idea has been applied by Stoekli *et al.* [7] to the binary adsorption of vapours using the Dubinin-Radushkevich isotherm.

Recently, Chang and Talu [8] studied theoretically and experimentally the performance of adsorbed methane storage cylinders under discharge conditions. Their experimental adsorption isotherms are shown in figure 1a. The analysis of these data on the basis of the potential theory results in a characteristic curve of adsorption on the carbon which is depicted in figure 1b. The constructed curve is temperature-independent, this fact corroborates the applicability of the theory. Saturation pressure and adsorbed molar volume,  $V_A$ , were calculated according to expressions proposed by Ozawa *et al.* [9].

In many cases, the theory can be generalized if an affinity coefficient,  $\beta$ , is used as shifting factor to bring the characteristic curves of all gases on the same adsorbent into a single curve. This is assumed to apply to all the species under consideration here. Based on the author's past

experience on light hydrocarbon adsorption, the liquid molar volume of the adsorbate at the normal boiling point was used as the affinity coefficient.

Although the functional form of the characteristic curve is adsorbent dependent, expressing the logarithm of the adsorbed phase volume,  $W$ , as a truncated series development of the scaled adsorption potential,  $\epsilon/\beta$ , provides good fitting of the experimental data [9]. A second-order polynomial is usually enough, as can be seen in figure 1b.

Multicomponent adsorption equilibrium prediction using the IAS method requires values of spreading pressure,  $\Pi$ , for adsorption of single gases. According to the potential theory, if this variable is scaled by  $V_A/\beta$  then it becomes a function of  $\epsilon/\beta$  only, and can be computed from a single curve for all intervening adsorbates:

$$A\Pi_i^* \equiv (V_A/\beta)_i A\Pi_i = \int_{\epsilon_i/\beta_i}^{\infty} W(\epsilon^*) d\epsilon^* \quad (i = 1, \dots, N). \quad (1)$$

If the development of  $\ln W$  as a power series of  $\epsilon/\beta$  accurately describes the experimental data, then eq. (1) suggests that  $A\Pi^*$  can also be expressed as a series development of the form

$$\ln(A\Pi_i^*/A\Pi_0^*) = \sum_{n=1}^{n=\infty} k_n (\epsilon_i/\beta_i)^n, \quad k_1 < 0, \quad (2)$$

where  $A\Pi_0^*$  is the value of  $A\Pi^*$  at saturation. As shown in figure 2a, a truncated second-order polynomial expansion describes very accurately the experimental data under consideration. Furthermore, the truncated series is easily invertible,

$$\epsilon_i/\beta_i = \frac{k_1}{2k_2} \left[ \sqrt{1 + (4k_2/k_1^2) \ln(A\Pi_i^*/A\Pi_0^*)} - 1 \right], \quad (3)$$

which is critical in speeding up the computations.

#### Discharge phase.

The model employed for the discharge phase is an extension to multicomponent adsorption of a prior model [10,11] that has been proven experimentally to describe successfully the discharge dynamics of methane adsorptive storage cylinders [8].

In an on-board storage reservoir the discharge rate is controlled by vehicle power requirements. This process is slow enough for pressure to be uniform within the cylinder and for the inexistence of intraparticle gradients. Hence, an equilibrium model can be employed at the particle level. Moreover, the cylinder is considered sufficiently long so that the small axial temperature gradient induced by the front and rear faces has negligible impact on the overall dynamics. These assumptions drastically reduce the spatial dimensionality of the problem, since only the radial profile needs to be taken into account. The implication of these assumptions on model performance is discussed to further length elsewhere [10].

The differential material balance for component  $i$  on a cylindrical shell element of the reservoir located at radial position  $r$ , can be written as

$$\epsilon \frac{\partial c_i}{\partial t} + \rho_b \frac{\partial q_i}{\partial t} - \frac{\epsilon}{r} \frac{\partial}{\partial r} \left( r D_{e,i} c \frac{\partial y_i}{\partial r} \right) + y_i F = 0 \quad (i = 1, \dots, N), \quad (4)$$

where  $c_i$  and  $q_i$  are the concentrations in gas and adsorbed phase, respectively,  $y_i$  is the mole fraction in gas,  $\epsilon$  and  $\rho_b$  are the porosity and bulk density of the carbon bed, and  $F(t, r)$  is the local contribution to the overall molar discharge rate per unit reservoir volume.

These balances are subjected to boundary conditions

$$\partial y_i / \partial r = 0 \quad \text{for } r = 0, R_0 \quad (i = 1, \dots, N), \quad (5)$$

where  $R_0$  is the cylinder radius.

As discharge proceeds, the consumed heat of adsorption is only partially compensated by the wall thermal capacity and by the heat transferred from the outside air. As a result, a radial temperature profile develops in the medium, the major temperature drop occurring at the centre of the bed. Given that pressure remains uniform within the cylinder, the temperature profile induces radial concentration gradients in both adsorbed and gas phases. The latter tend to be lessened by bulk diffusion which is taken into account in the third term of eq. (4).

Accordingly, the local contribution  $F$  must also vary along  $r$  in order to ensure uniform pressure in the cylinder and to satisfy the following integral constraint over the cross section of the cylinder:

$$2\pi L \int_0^{R_0} F(t, r) r dr = Q, \quad (6)$$

where  $L$  is the cylinder length and  $Q$  is the imposed overall molar discharge rate.

The energy equation, applied to the same differential volume, yields

$$\left[ \rho_b C_s + C_g (\varepsilon c + \rho_b q) \right] \frac{\partial T}{\partial t} - \varepsilon \frac{dP}{dt} + \rho_b \sum_i (-\Delta H)_i \frac{\partial q_i}{\partial t} - \frac{1}{r} \frac{\partial}{\partial r} \left( r \lambda_e \frac{\partial T}{\partial r} \right) = 0, \quad (7)$$

where  $C_s$  and  $C_g$  are the carbon and gas heat capacities, respectively,  $T$  is temperature,  $P$  is gas pressure,  $-\Delta H_i$  is the heat of adsorption for species  $i$ , and  $\lambda_e$  is the effective thermal conductivity of the carbon bed.

Equation (7) is subjected to boundary conditions

$$\partial T / \partial r = 0 \quad \text{for } r = 0, \quad (8)$$

$$\left( 1 + \frac{e_w}{2R_o} \right) e_w C_w \frac{\partial T}{\partial t} + \lambda_e \frac{\partial T}{\partial r} = \left( 1 + \frac{e_w}{R_o} \right) h_w (T_{\text{amb}} - T) \quad \text{for } r = R_o. \quad (9)$$

The latter condition is an energy balance on the steel cylinder wall, it cannot be neglected due to its large thermal capacity. Symbols  $e_w$ ,  $C_w$  and  $h_w$  represent wall properties (thickness, volumetric heat capacity, and natural convection heat transfer coefficient at the external surface, respectively) and  $T_{\text{amb}}$  is ambient temperature.

#### Charge phase.

Heat effects during the charge phase are neglected mainly because adequate solutions have been proposed to eliminate them. For example, at a refuelling station the gas can be cooled before charging the reservoir or an external NG recycle loop can remove the heat and reject it to the environment across an air-cooled heat exchanger [12]. Alternatively, fleet vehicles can be charged over a long period, e.g. overnight, which provides enough time to dissipate the heat of adsorption. The interested reader is referred to Mota [10] for rigorous modeling work on heat effects in the fast charge of ANG storage cylinders.

According to these assumptions, a lumped-based model can be adopted for the charge phase. At the end of the discharge, the residual amount of each component left in storage per unit reservoir volume is computed from

$$S_i = (2/R_o) \int_0^{R_o} (\varepsilon c_i + \rho_b q_i) r dr \quad \text{at depletion} \quad (i = 1, \dots, N). \quad (10)$$

Then, the following set of lumped material balances is solved in order to compute the new discharge initial conditions:

$$\varepsilon c_i + \rho_b q_i = S_i + z_i F_c \quad \text{with } P = P_{\text{charge}} \quad \text{and } T = T_{\text{amb}} \quad (i = 1, \dots, N), \quad (11)$$

where  $F_c$  is the amount of gas admitted to the cylinder during charge and  $z_i$  is its mole fraction composition.  $F_c$  is an unknown which is computed along with the new initial discharge conditions.

## RESULTS AND DISCUSSION

Unfortunately, due to lack of space most of the paper has been spent describing the theoretical model, leaving room for a limited amount of results. The discharge phase model is validated for single-gas adsorption by comparison with the experimental temperature history in an adsorbed methane cylinder during discharge. As shown in figure 2b, model results are in close agreement with the experimental data.

Multicomponent discharge dynamics is summarized in figures 3a and 3b. It is a complex function of the adsorption potential of each component and its mole fraction in the charge gas. Depletion pressure is 1.4 atm while charge pressure is 35 atm. The discharge flow rate considered, 6.7 l/min, produces a methane discharge duration of about 4 hours under non-isothermal conditions. Table 1 lists the values of the main parameters employed in the numerical simulations. The gas composition considered in this study is given in table 2, it characterizes the NG from the Hassi R'Mel well supplying Portugal.

The net deliverable capacity is measured in terms of dynamic efficiency, which for component  $i$  is defined as

$$\eta_i = \frac{\text{amount of species } i \text{ delivered under dynamic conditions}}{(\text{amount of pure methane delivered isothermally}) \cdot z_i}, \quad (12)$$

where  $z_i$  is its mole fraction in the charge gas (table 2). This way, the  $\eta$  values converge to a common point at the cyclic steady state (figure 3a). The dynamic efficiency decreases gradually with the number of cycles to the cyclic steady-state value, although it attains a maximum at intermediate cycles for the higher hydrocarbons if their mole fractions in the charge gas are high enough. Until steadiness is reached, the total hydrocarbon capacity loss ( $C_1-C_5$ ) depends linearly on the logarithm of the number of cycles. This is agreement with the experimental observations of Golovoy and Blais [13] for 100 cycles of operation of an ANG cylinder.

The temperature and mole fractions shown in figure 3b are lumped values obtained from averaging the variable over the cross section of the cylinder. The same figure shows that the discharge duration is reduced as the number of cycles is increased since the micropore volume is gradually occupied by the higher hydrocarbons which tend to remain adsorbed at depletion pressure. The temperature history is approximately linear, because the discharge is carried out at constant molar rate, and is nearly insensitive to the cycle number.

## CONCLUSIONS

A detailed mathematical model has been developed in order to study the impact of NG composition on cycling efficiency of ANG reservoirs. Although the model has been applied to a single NG, other gas compositions should produce the same qualitative behaviour. The results emphasize the need to identify and evaluate economical means of removing the contaminants from the gas stream before charge. The solution could be either a gas clean-up system installed at the refueling station [4,12] or a guard bed placed in front of the on-board storage reservoir [14].

## ACKNOWLEDGEMENTS

Financial support received from PRAXIS XXI (PCEX/C/QUI/109/96) and from FLAD is gratefully acknowledged.

## REFERENCES

1. N. D. Parkyn and D. F. Quinn, In *Porosity in Carbons* (Edited by J. Patrick), pp. 291–325. Edward Arnold, London (1995).
2. O. Talu, Proceedings 4th International Conference on Fundamentals of Adsorption, Kyoto, Japan, pp. 655–662 (1993).
3. T. L. Cook, C. Komodromos, D. F. Quinn and S. Ragan, In *Carbon Materials for Advanced Technologies* (Edited by T. Burchell). Elsevier, in press.
4. M. Sejnoha, R. Chahine, W. Yaïci, and T. K. Bose, Paper presented at AIChE Meeting, San Francisco (1994).
5. S. Brunauer, *The adsorption of gases and vapours*. Oxford University Press, Princeton (1945).
6. A. L. Myers and J. M. Prausnitz, *AIChE J.* **11**, 121–127 (1965).
7. F. Stoeckli, D. Wintgens, A. Lavanchy, and M. Stöckli, *Adsorp. Sci. Technol.* **15**, 677–683 (1997).
8. K. J. Chang and O. Talu, *Appl. Thermal Engng* **16**, 359–374 (1996).
9. S. Ozawa, S. Kusumi, and Y. Ogino, *J. Coll. Int. Sci.* **56**, 83–91 (1976).
10. J. P. B. Mota, *Modélisation des transferts couplés en milieux poreux*, Ph.D. Thesis, Institut National Polytechnique de Lorraine, France (1995).
11. J. P. B. Mota, A. E. Rodrigues, E. Saadjan, and D. Tondeur, *Carbon* **35**, 1259–1270 (1997).
12. W. E. BeVier, J. T. Mullhaupt, F. Notaro, I. C. Lewis, and R. E. Coleman, Paper presented at 1989 SAE Future Transportation Technology Conference and Exposition, Vancouver (1989).
13. A. Golovoy and E. J. Blais, In *Alternate Fuels for Special Ignition Engines*, p. 47. SP-559 SAE Conference Proceedings, Warrendale, PA 15096 (1983).
14. T. L. Cook, C. Komodromos, D. F. Quinn, and S. Ragan, Paper presented at Windsor Workshop on Alternative Fuels, Toronto (1996).

$C_g = 355.5 \text{ atm}\cdot\text{cm}^3\cdot\text{mol}^{-1}\cdot\text{K}^{-1}$	$P_{\text{depletion}} = 1.4 \text{ atm}$
$C_s = 10.38 \text{ atm}\cdot\text{cm}^3\cdot\text{g}^{-1}\cdot\text{K}^{-1}$	$R_o = 10 \text{ cm}$
$C_w = 38.68 \text{ atm}\cdot\text{K}^{-1}$	$T_{\text{amb}} = 20 \text{ }^\circ\text{C}$
$e_w = 0.55 \text{ cm}$	$\varepsilon = 0.5$
$L = 74 \text{ cm}$	$\lambda_e = 1.26 \text{ atm}\cdot\text{cm}^2\cdot\text{min}^{-1}\cdot\text{K}^{-1}$
$P_{\text{charge}} = 35 \text{ atm}$	$\rho_b = 0.481 \text{ g}\cdot\text{cm}^{-3}$

Table 1: Data employed in numerical simulations.

Component	CH <sub>4</sub>	C <sub>2</sub> H <sub>6</sub>	C <sub>3</sub> H <sub>8</sub>	C <sub>4</sub> H <sub>10</sub>	C <sub>5</sub> H <sub>12</sub>	N <sub>2</sub>
Mole fraction	0.840	0.076	0.020	0.007	0.003	0.054

Table 2: Composition of natural gas from the Hassi R'Mel well (Algeria) supplying Portugal.

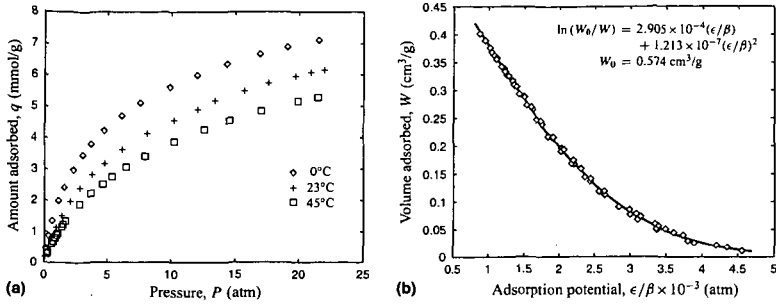


Figure 1: Methane adsorption on an activated carbon. (a) Experimental isotherms reported by Chang and Talu [8]; (b) corresponding characteristic curve of adsorption plotted according to the potential theory.

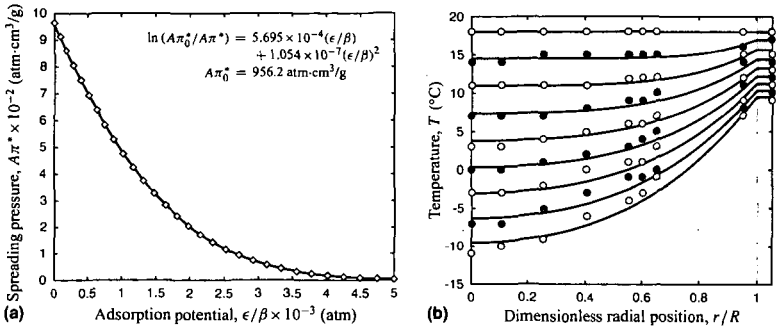


Figure 2: (a) Spreading pressure as a function of scaled adsorption potential for the carbon under study. (b) Radial temperature profiles in an adsorbed methane cylinder as a function of time during discharge. Comparison between experiments [8] (points) and model predictions (lines). Sampling interval = 20 min;  $L = 74$  cm,  $R = 10$  cm, carbon weight = 15.78 kg, discharge rate = 6.7 l/min, charge pressure = 21 atm, depletion pressure = 1.6 atm.

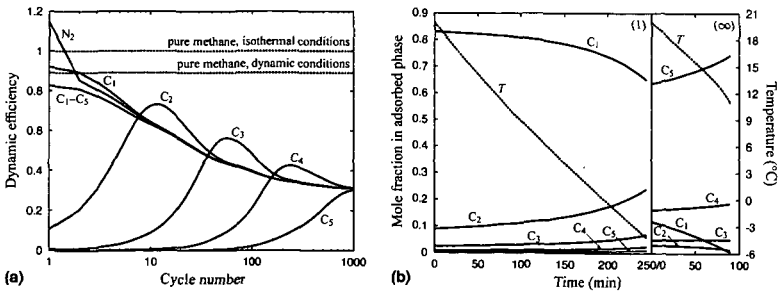


Figure 3: (a) Dynamic efficiency,  $\eta_i$ , as a function of cycle number for an ANG cylinder. (b) Histories of temperature and mole fractions in adsorbed phase for (1) first and ( $\infty$ ) cyclic steady-state discharges in an ANG cylinder.